

## CHAPTER 2 BACKGROUND

### 2.1 Overview

As discussed earlier, cesium and silicon are ideally poised as model systems for the study of surface phenomena and metal-semiconductor interfaces in general and in contrast with other transition metal semiconductor interfaces they are easier to understand due to their simpler interactions with the substrate. In order to gain an understanding of saturation coverage, metallization and Schottky-barrier formation, it is necessary to study the chemical bonds and electron localization at the surface and also relate them to the their surface structures. The monolayer saturated films provide an ideal regime for the study of these properties at the atomic level and understand how they relate to properties for interfaces with higher coverage or with the bulk structure.

In the following sections we discuss the structure and properties of bulk silicon and its various bulk-terminated and surfaces. This will be followed by a background of studies on the reconstructions of each of these surfaces and a summary of studies of cesium adsorption on these surfaces.

### 2.2 The Ideal Silicon Crystal And Bulk Termination

The bulk structure of silicon, shown in Figure 2.1 is a diamond lattice<sup>1</sup>, consisting of covalent  $sp^3$  hybridized bonds. It has a face-centered cubic lattice with an edge length of  $a = 5.43 \text{ \AA}$  and a two atom basis:  $\left\{ 0, \frac{5.43\text{\AA}}{4}(\hat{x} + \hat{y} + \hat{z}) \right\}$  which yields an inter-atomic spacing of  $2.35 \text{ \AA}$ .

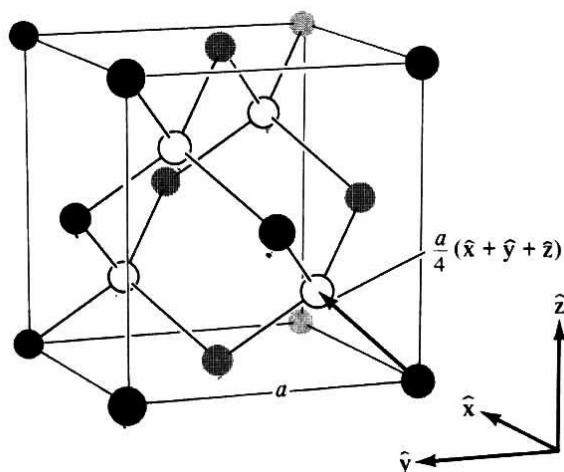


**Figure 2.1** Zinc blende structure, which is equivalent to diamond or Silicon structure if all atoms were identical<sup>1</sup>. The white spheres denote atoms within the cube and the black atoms lie on the surface of the cube.

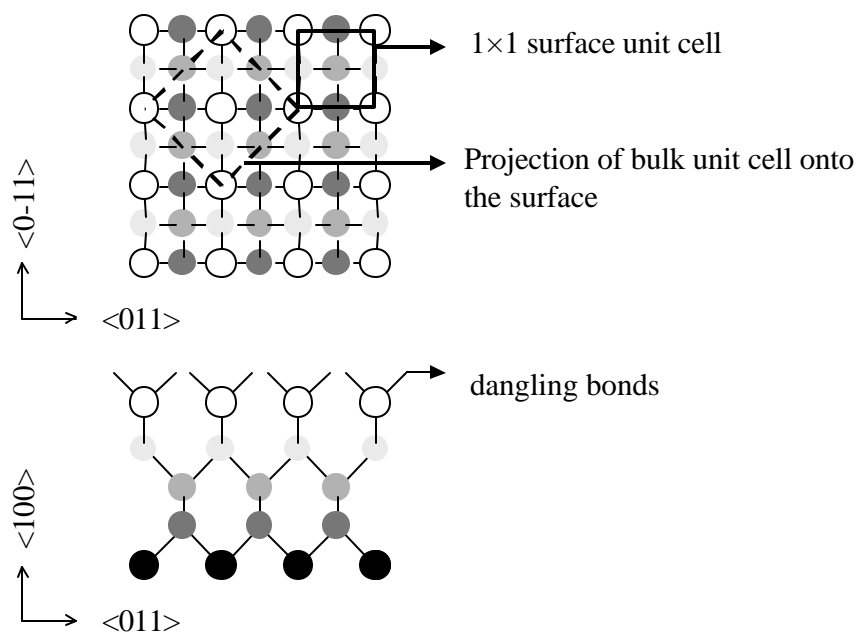


**Figure 2.2** Top and side views of the unreconstructed Si(100) surface. The topmost atoms are white and the deeper atoms are shown in progressively darker shades.

Silicon naturally cleaves along the Si(111) plane. Silicon crystal wafers are usually cut to expose the Si(100) and Si(111) surfaces. The positions of atoms in the bulk structure gives us a basic reference system for coverage measurements for both the Si(100) and Si(111) surfaces. The ideally terminated surface has surface atoms in the same positions as they would have in the bulk. This allows us to calculate the number of surface atoms per unit area. The areal density is used as a basis for defining a monolayer (ML) for each surface of the silicon crystal.

The bulk-terminated Si(100)<sup>2</sup> surface has an exposed face that resembles the top square of the cube in Figure 2.1. This is shown in greater detail in Figure 2.2. Each surface atom gives rise to two dangling bonds. In each repeating projected unit cell on the surface, there are two atoms, which works out to  $6.78 \times 10^{14}$  atoms/cm<sup>2</sup>. This is defined as a coverage of one ML and is used as the reference for cesium coverage of the Si(100) surface.

Figure 2.3 shows two planes passed through a face centered cube (FCC) with both planes having the normal vector (1,1,1). If two such cubes were stacked, one atop the other, the two gray triangles will fit together to form one rhomboid cell. This cell consists of four rhomboid unit cells of the FCC(111) plane containing one atom each shown in Figure 2.4. The areal density corresponding to one ML for this face is  $7.83 \times 10^{14}$  atoms/cm<sup>2</sup>.

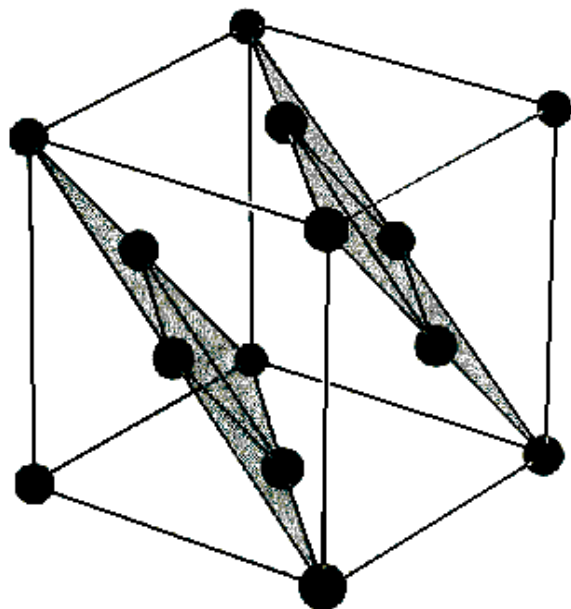


Figure 2.3 A unit cell for the (111) plane of an FCC (or diamond structured) crystal.<sup>1</sup>

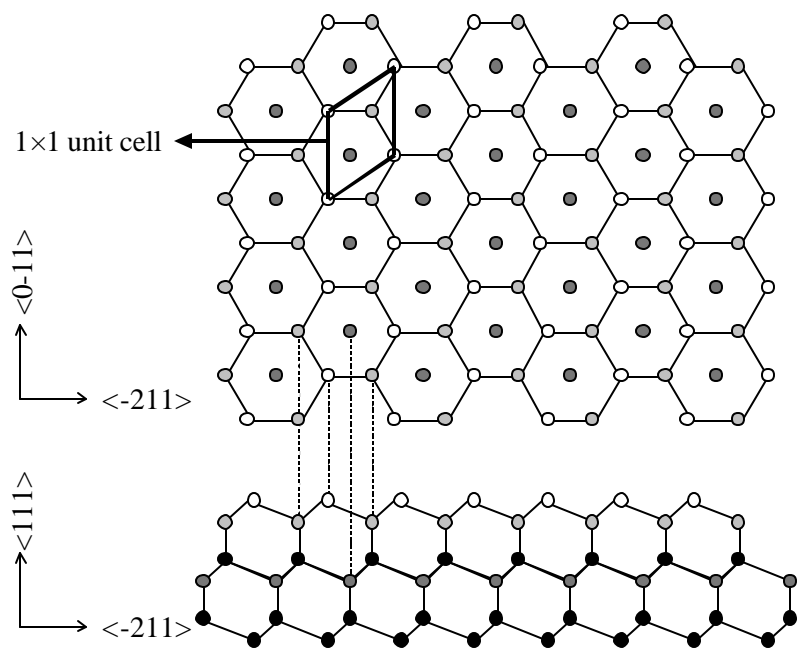


Figure 2.4 Top and side views of the unreconstructed Si(111) surface. The topmost atoms are white and the deeper atoms are shown in progressively darker shades.

In practice, the surfaces of real semiconductor crystals are never simple bulk terminations. Generally, the outermost layer or layers move closer to the bulk. In most cases, more complex reconstructions of the surface also occur.<sup>3</sup> The various faces of silicon have numerous known reconstructions.<sup>4,5</sup>

In semiconductors, interatomic bonds are highly localized unlike in metals and interactions between the unsatisfied dangling bonds of the surfaces are less significant in comparison. Theoretical models of alkali metals on GaAs predict, that surfaces like Cs/GaAs and K/GaAs are Mott-Hubbard insulators.<sup>6,7,8,9,10,11,12,13</sup> A surface with a silicon substrate offers an interesting point of comparison. Si has different inter-atomic distances at the surface depending on the cleavage plane. Silicon also offers a wide variety of surface reconstructions, whose study can further improve our understanding and at the same time serve as a test for theoretical calculations.

In ideal bulk-terminated Si surfaces, there are unfulfilled dangling bonds directed normal to the surface. In the Si(100) surface, each surface atom loses two of its four nearest-neighbors leaving two others free and in Si(111) only one nearest-neighbor is lost leading to only one free dangling bond per atom. Thus the areal density of dangling bonds for the unreconstructed Si(111) surface is more than twice of that of the Si(100) surface.

The dangling bonds produce charge distributions that are energetically unfavorable. Relaxation and reconstruction are a means of minimizing the energy and

saturation of the broken bonds on the surface. The free dangling bonds can either interact with each other or with the backbonds, pointing back towards the bulk. Reconstruction-induced pairing of electrons causes splitting of bands and a filling in of the lower energy states. A simplistic view may lead one to think that the surface becomes semiconducting or insulating. In reality though the changes in the two-dimensional surface band structure are complex. The Si(111)  $7\times 7$  surface is classified as metallic due to a partially-filled band which crosses the Fermi-level, the Si(100)  $2\times 1$  is semi-conducting and the Cs/Si(111)( $\sqrt{3} \times \sqrt{3}$ )R30°-B is an insulating surface.

## **2.3 The Cs/Si(100) Interface**

### **2.3-a Overview of the Si(100) surface**

The bulk-terminated Si(100) surface illustrated in Fig 2.3, has a  $1\times 1$  structure with each surface atom having two dangling bonds at a  $55^\circ$  angle from the surface normal. Such a surface is highly reactive and unstable. Many feasible ways of minimizing the energy suggest themselves. In general interactions can occur between 1) bonds belonging to the same atom 2) bonds of neighboring atoms and 3) surface and back bonds. There are a large number of dangling bonds per unit area on this surface as compared to the Si(111) face, so the reconstructions can be expected to exhibit a comparatively short range order.

### 2.3-b The Si(100)-2×1 Reconstruction

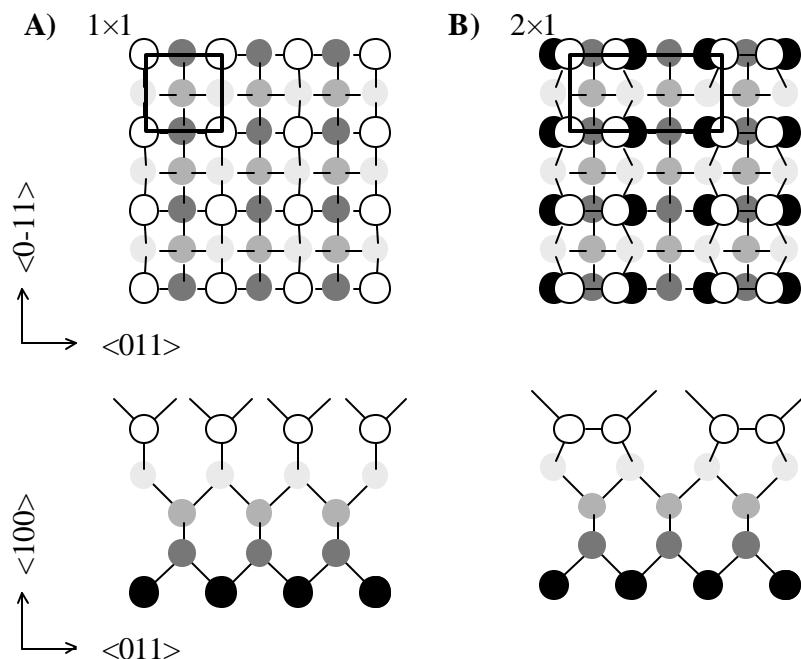


**Figure 2.5** Top and side view of the symmetric dimer model of the Si(100)-2×1 surface. Atoms farther away are also indicated by how the bonds overlap or underly the atoms. A) The 1×1 bulk termination, showing 2 dangling bonds per surface atom. B) The 2×1 reconstruction shown with symmetric dimers.

A very simple reconstruction to minimize the energy of the surface is shown in Figure 2.5 B, where pairs of atoms move closer together to form dimers. This simple structure gives rise to rows of dimers separated by valleys. The energy can be minimized further, by introducing alternating tilts in the adjacent dimers in a row. This gives rise to two asymmetric structures as shown in Figure 2.6.

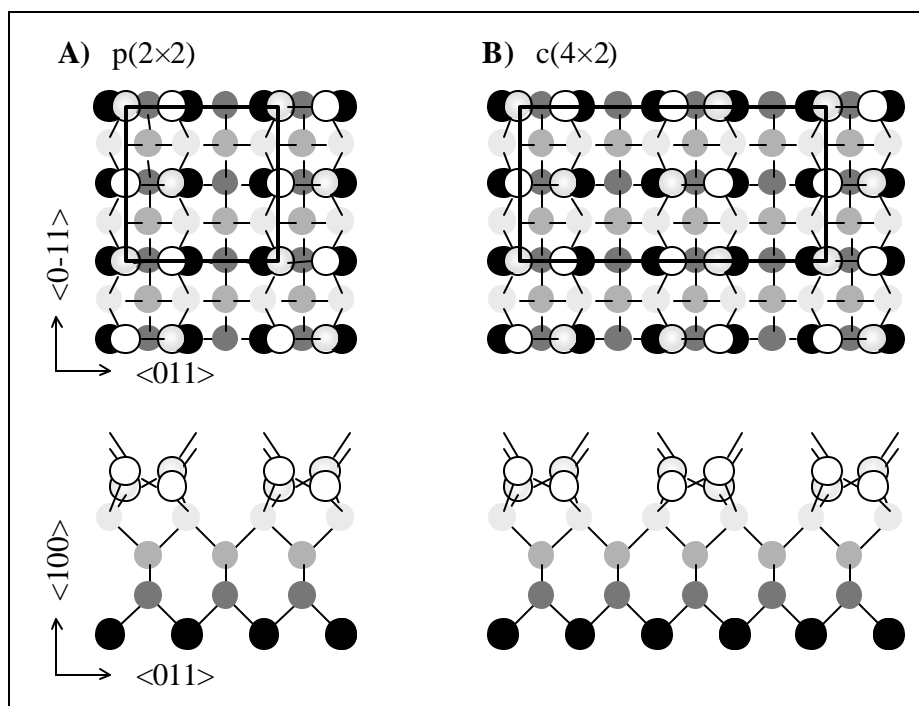


**Figure 2.6** Top and schematic view of atoms in the Si(100) surface. A unit cell is outlined for each reconstruction. A) The  $p(2 \times 2)$  asymmetric model where the dimer tilts in adjacent rows are in phase B) The  $c(4 \times 2)$  asymmetric model where the dimer tilts in adjacent rows are out of phase This structure is known to be stable below  $200^\circ\text{K}$  and is called the  $c(4 \times 2)$  phase. (The “c” stands for centered to indicate that the unit cell includes a point at its center which is equivalent to the points at the corners). C) and D) A transverse view of both reconstructions. The grey circles represent atoms closer to the bulk, and white circles represent atoms higher up.

The first structural evidence from Low Energy Electron Diffraction (LEED) data<sup>14</sup> pointed to a symmetric dimer with a  $2 \times 1$  symmetry. Subsequent studies of the surface using Angle Resolved Photoemission Spectroscopy (ARPES) found completely filled states and a band gap implying that the surface was a semiconductor. Theoretical band structure calculations contradicted this by yielding a conducting surface for symmetric dimers. Chadi<sup>15</sup> first introduced the idea of buckling or tilted dimers when he



observed that similar calculations could yield a semiconducting surface for buckled structures. There are two ways the buckling can take place as shown in Figure 2.6. In one scheme the buckling between adjacent dimer rows can be in phase  $p(2\times 2)$  or they can be out of phase  $c(4\times 2)$ . The energy of the  $2\times 2$  structure is slightly higher than the other by an easily bridgeable gap at room temperature, and at least on theoretical grounds, both structures are expected to coexist.

Experimental evidence for the reconstructions outlined above, are complicated by step defects and time-averaging. The bulk structure of silicon has atoms with different bond directions at different levels. This means that the dimers on a particular face revealed due to steps will have a different orientation from the dimers on any other face an odd number of atomic layers away (and the same orientation as those on steps an even number of layers away).

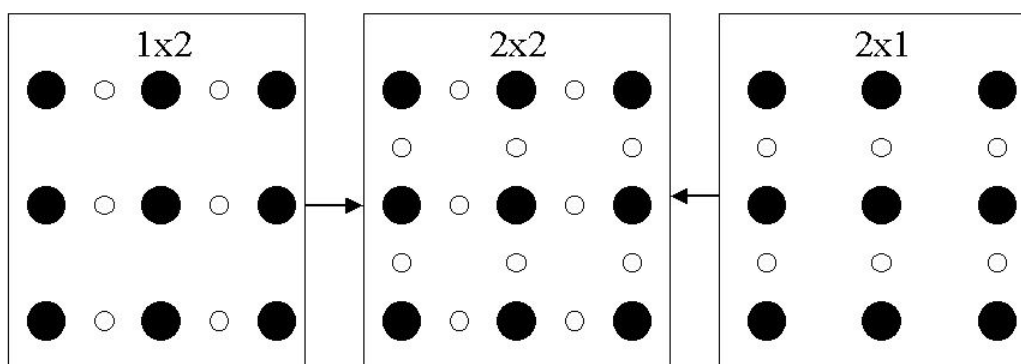


**Figure 2.7** Diffraction patterns from Si(100)  $2\times 1$  (left) and from Si(100)  $1\times 2$  (right). Both are present in most Si(100) samples. They overlap to give an apparent  $2\times 2$  pattern (middle). The half order spots (shown in white) are only present in half the sample, so they have about half the intensity they would otherwise have and are fainter than the integer order spots (shown in black).

When LEED or any other area averaging technique is used to determine the symmetry of a face, it generally averages over many of these steps, thus, instead of seeing a simple  $2\times 1$  pattern, one sees the superposition of a  $2\times 1$  pattern with a  $1\times 2$  pattern as shown in Figure 2.7. This simplified picture does not even address the issue of whether the single domain surface is  $4\times 2$  or  $2\times 2$  which complicates the LEED image further.

Another complication is the issue of time-averaging. Since buckled dimers can equally well be tilted in either direction, they can oscillate quite rapidly between different states. This means that most probes, which take time averages cannot resolve the oscillations, and see symmetric dimers, instead of oscillating buckled dimers. Indeed, simulations by Shkrebtii *et al.*<sup>16</sup> found oscillations with periods on the order of a picosecond. Their simulations agree for the most part with the STM study of Tromp *et al.*<sup>17</sup> which found a variety of different dimer structures present on most room temperature Si(100) faces. Similarly, Landemark *et al.*<sup>18</sup> found via photoelectron spectroscopy that the surface is entirely covered with buckled dimers which lose long-range order when heated to room temperature. (Hamers *et al.* report that the  $2\times 1$  LEED pattern is replaced by a sharp  $c(4\times 2)$  pattern at  $80^\circ\text{K}$ , implying that the dimers have stopped oscillating and are “frozen” into a buckled configuration.<sup>19</sup>) For purposes of this work, for the sake of simplicity the surface will be referred to as Si(100)  $2\times 1$ , leaving some of the details are unspecified.

### 2.3-c Prior Investigations of the Cs/Si(100) 2×1 Interface

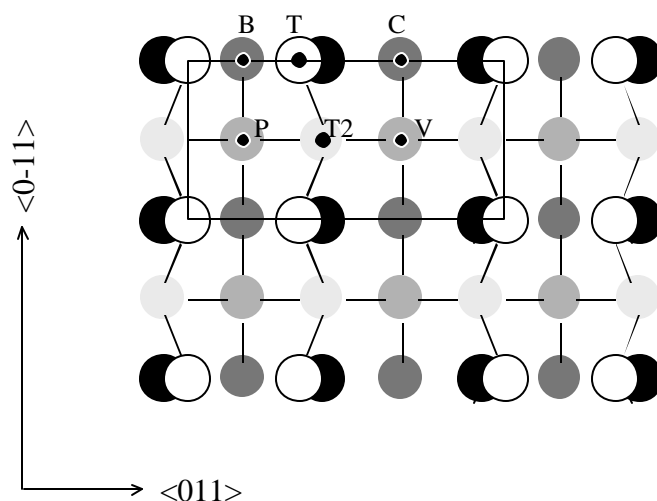


**Figure 2.8<sup>20</sup>** Potential binding sites for Cs on Si(100) 2×1. White circles are atoms in the first layer, gray circles are atoms in the 2<sup>nd</sup> layer, and black dots show the possible binding sites: P: the Pedestal site, B: the Bridge site, T: on Top of one of the dimer atoms, T2: on Top of one of the atoms in layer 2, C: in the Cave (above the deepest exposed atom), and V: the Valley site. (A 2×1 unit cell is drawn in.)

There have been numerous studies of the Cs/Si(100) 2×1 system at various coverages and temperatures. There is no widely accepted nomenclature for the possible adsorption sites for cesium, but a standard can be extracted from the published literature. Directly between two atoms in a dimer is the Bridge site (B). Directly above one of the surface atoms is the Top site, or the T1 site (on top of an atom in layer 1). In the deep space between two dimers is the Cave (C) or T4 site, which sits directly over an exposed

atom in the 4<sup>th</sup> layer of the silicon. In the center of the square formed by two neighboring dimers is the Pedestal site (P). Directly over an atom in the 2<sup>nd</sup> layer is the T2 site. Between T2 sites are so-called Valley sites (V) or T3 sites. All the studies made to date predict that the cesium atoms will adsorb on or near one of the on-top sites, or the four sites of high symmetry on the Si(100) 2×1 surface (See Figure 2.8).

Some of the earliest work on the Cs/Si(100) interface was carried out by Goldstein<sup>21</sup> and Levine<sup>22</sup> in the early 1970's because of interest in the Negative Electron Affinity (NEA) state of the O/Cs/Si(100). Goldstein observed an unchanged LEED pattern for the saturated Cs/Si(100) interface except for strengthened half-order spots (which made sense since cesium has a higher electron scattering cross section than silicon). It was also observed that cesium had to be dosed before the oxygen for the NEA surface to form properly, which suggested that the Cs/Si structure was the same as the O/Cs/Si structure. They proposed their surface model based on these key observations. They assumed that the lowering of the work function in the O/Cs/Si(100) surface arose from a Cs-O surface dipole. Given their electronic properties one can assume that Cs gives up an electron and that oxygen tends to attract electrons (though recent work<sup>23</sup> has found that there is minimal charge transfer between the Cs and the substrate). This led them to propose that the oxygen must bond in a site relatively deep into the surface of the silicon like the cave site, and that the cesium must be relatively high above the surface (see Figure 2.8). This was called the Levine model where the oxygen atoms sit in cave sites, and the cesium atoms are in pedestal sites.

The Levine model yields a total coverage of one cesium atom per two surface silicon atoms or 0.5 Monolayer (ML). This means that each unit cell on the interface has an odd number of valence electrons contributing to the surface states, which constitute a half-filled band (since cesium has only one 6S valence electron). Thus the interface is expected to be conducting. This was indeed supported by core and valence electron photoemission studies by Mangat *et al.*<sup>23</sup> and Chao *et al.*<sup>24</sup> and by STM studies of Xu *et al.*<sup>25</sup> (Although Chao *et al.* concluded two adsorption sites for the cesium, which is taken as a partial refutation of the Levine model by some).

Other work, however, cast doubt on the Levine model. Enta *et al.* using angle-resolved ultraviolet-photoelectron-spectroscopy (ARUPS), observed that both the K/Si(100)  $2\times 1$ <sup>26</sup> and the Cs/Si(100)  $2\times 1$ <sup>27</sup> interfaces are semiconducting. This, along with their own low energy electron diffraction (LEED) and x-ray photoelectron diffraction (XPD<sup>28</sup>) lead Abukawa and Kono to propose their model of 1 monolayer Cs coverage for both interfaces.<sup>29,30,31</sup> In this model (see Figure 2.9), the cesium atoms are adsorbed on both the pedestal and the bridge sites. This gives an even number of valence electrons per unit cell, and is consistent with a semiconducting surface.

Experimental support for the Abukawa and Kono model has come from different sources. LEED I-V<sup>32</sup> studies carried out by Hamamatsu *et al.*<sup>33</sup> strongly supported the Abukawa and Kono model. Partial support also came from techniques, which found that cesium had two different bonding states on the saturated surface. Kennou *et al.*<sup>34</sup> performed thermal desorption spectroscopy (TDS) of the interface and found two primary

desorption peaks near 550°K and 775°K. Similarly, Chao *et al.*<sup>24</sup> studied the interface with core and valence photoelectron spectroscopy and concluded that the surface had two adsorption sites. It should be noted that the presence of two binding sites in itself does not imply that all available sites are occupied. It is possible to propose models with an epitaxial arrangement of the Cs atoms on both binding sites, which yields a 0.5 ML coverage. In fact Kennou *et al.* report a saturation coverage of only 0.75 ML (based on rate calculations), and Chao *et al.* report that the interface is metallic. (Chao *et al.* concluded that the silicon dimers in the cesium saturated surface are asymmetric, while Hamamatsu *et al.* concluded that the dimers are symmetric.)

Numerous other experimental and theoretical studies have been used to support either the Levine or the Abukawa and Kono models for Cs/Si(100) 2×1 saturation coverage, but many focus on the other alkali-metals. Unfortunately, the analogies are not always convincing. The interface most commonly associated with Cs/Si is K/Si. Potassium, however, has been observed<sup>35</sup> via TDS to adsorb as bulk islands stable up to 370 °K on the Si(100) 2×1 surface. This suggests that various reports of 1 or 0.5 monolayers for saturation coverage are neither conclusive, nor similar to the cesium interface, where no bulk island formation has been reported. The other alkali-metals are not of great use in analyzing the cesium interface either.<sup>36,37</sup>

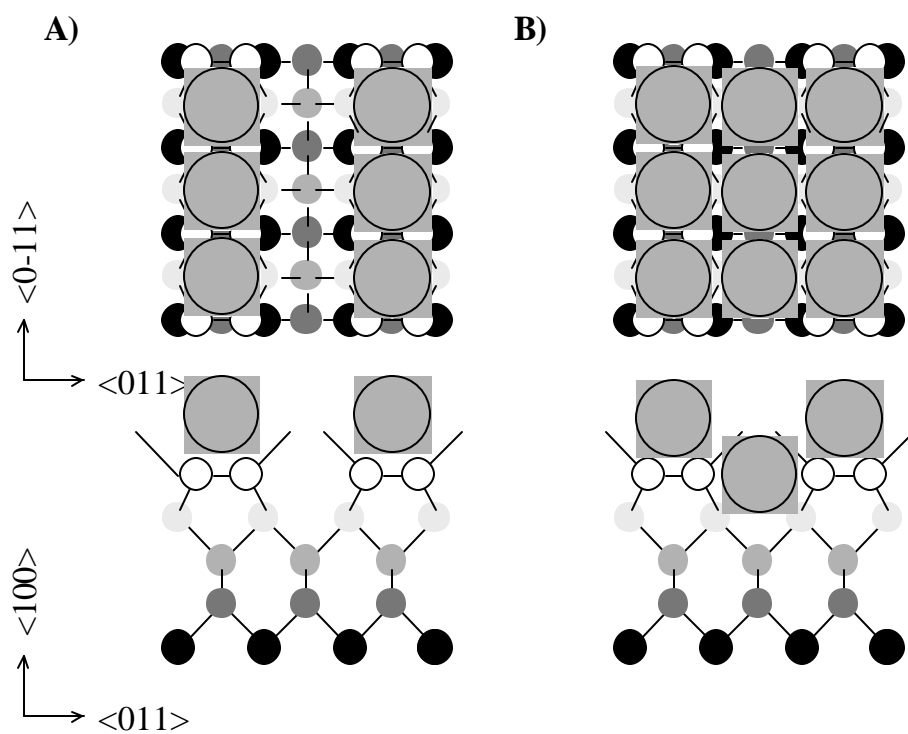


**Figure 2.9** The Levine and Abukawa & Kono models. A) The Levine model with 0.5ML of Cs, showing gray cesium atoms. Above: Top view, Below: cutaway view. B) The Abukawa and Kono model of Cs/Si(100) 2x1 showing 1 monolayer of coverage, with gray Cs atoms. Above: Top view, Below: Side view.

There have only been two studies which might have yielded absolute coverage for the Cs/Si(100)-2×1 interface. Xu *et al.*<sup>25</sup> carried out STM studies of the interface, but could not resolve the detailed atomic positioning (they cited intrinsic difficulty imaging the interface mentioned earlier). They suggested that while the cesium layer is conducting, the silicon substrate below is still semiconducting and that may explain the contradictory results for various probes with less elemental specificity or depth resolution. Smith *et al.*<sup>38</sup> reported via hydrogen beam Medium Energy Ion Scattering (MEIS) studies that the saturation coverage is  $0.97 \pm 0.05$  ML. Mangat and Soukiassian<sup>23</sup> have found that very small contaminants can cause additional adsorption, and Soukiassian suggested,<sup>39</sup> that the hydrogen in the MEIS beam, or in the beam residue may have contaminated the sample. It is also possible that contaminants like oxygen in a defective experimental set up may actually drive up the saturation coverage of Cs. This is borne out by our Auger studies, which found evidence of greater cesium being adsorbed with no clear saturation limit for samples with a high degree of contamination.

In these studies, helium beam Rutherford backscattering spectrometry (RBS) is used for the Cs/Si(100) 2×1 interface. The helium beam is unreactive, and thus avoids the potential contamination problems associated with the earlier hydrogen beam MEIS study. Monitoring of contaminant levels in this study is a check against impurity induced adsorption. Meanwhile, RBS provides an absolute coverage of the amount of cesium on the interface. The measured coverage is independent of any particular structural model and depends only on the measured quantities and known collision cross-sections. It



should be emphasized that this model independence distinguishes it from LEED I-V, TDS, ARUPS, XPD, STM and all other probe techniques, which can be brought to bear on this interface. Firmly establishing the absolute coverage, however, will be a key component of establishing the exact surface structure. Particularly since the two primary structural models predict very different coverages.

## **2.4 The Cs/Si(111) 7×7 Interface**

### **2.4-a Overview of the Si(111) surface**

The (111) planes of Si can be thought of as double layers, which are attached to each other by bonds, one per atom, perpendicular to the layers. Within the double layer a mesh of the remaining tetrahedral bonds (three per atom) connect the atoms in 3-fold symmetric coordination. Cleavage along the (111) plane results in the breakage of the bonds that connect the two double-layers, see Figure 2.10. A dangling  $sp^3$  hybrid orbital per surface adatom is left normal to the top double layer.

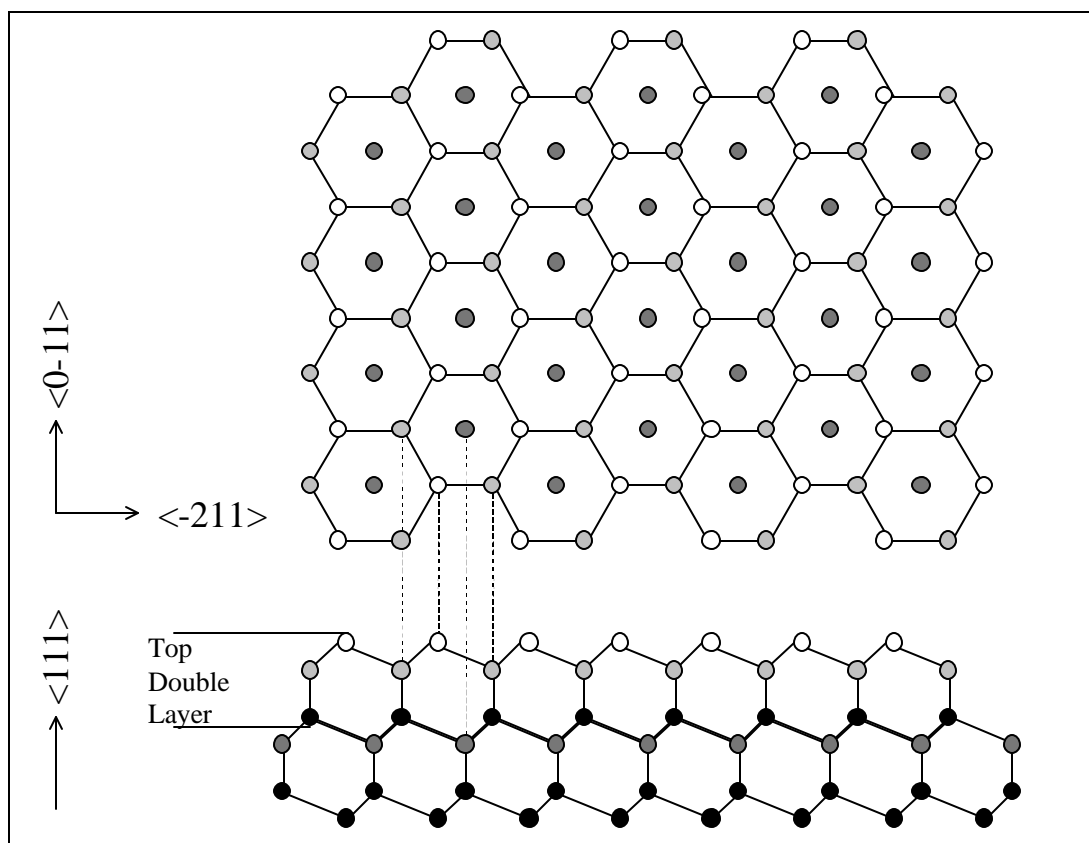


**Figure 2.10** The top and side views of an ideally terminated Si(111) surface which preserves the bulk structure. The surface unit cell is indicated by bold dotted lines.

The unreconstructed surface thus consists of parallel dangling bonds, one per surface unit cell (formed by projecting the bulk structure onto the surface) as shown in Figure 2.10. These dangling bonds are highly energetic and the clean surface seeks to rearrange in such a way as to reduce their number. In contrast with the Si(100) surface, since there is only one bond per surface atom, the surface thus has the tendency for reconstructions having comparatively long-range order to minimize energy.

The simplest reconstruction of Si(111) surface is a  $2\times 1$  reconstruction, whose structure has been determined by LEED. The reconstruction involves rearranging atoms from the hexagonal rings (normally six per ring) to form alternating rings with five and seven atoms. This arrangement buckles the surface, and brings the dangling orbitals closer to each other. Although the number of surface bonds remains the same the energy is lowered due to weak  $\pi$  bonding interaction between them.

#### **2.4-b The Si(111) $7\times 7$ Reconstruction**

The most stable reconstruction of a silicon crystal has a  $7\times 7$  unit cell formed on the Si(111) surface. However this surface can only be obtained by annealing the Si(111)  $2\times 1$  surface.<sup>14</sup> The formation of the Si(111)  $7\times 7$  structure primarily involves the removal of 49 dangling-bonds by using dimers, adatoms, and stacking faults<sup>40, 41</sup> as shown in Figure 2.11. A stacking fault formation is highly energetic, therefore the surface can only be produced by annealing at high-temperature, even though the resulting surface is far more stable. The large number of atoms per the double-layered  $7\times 7$  cell cell, has made the determination of the  $7\times 7$  structure a complicated task. The Si(111)  $7\times 7$  surface has been attacked by every surface tool, primarily because of the technological importance of silicon, and the determination of the detailed structure of the Si(111)  $7\times 7$  surface was a significant achievement for surface science.

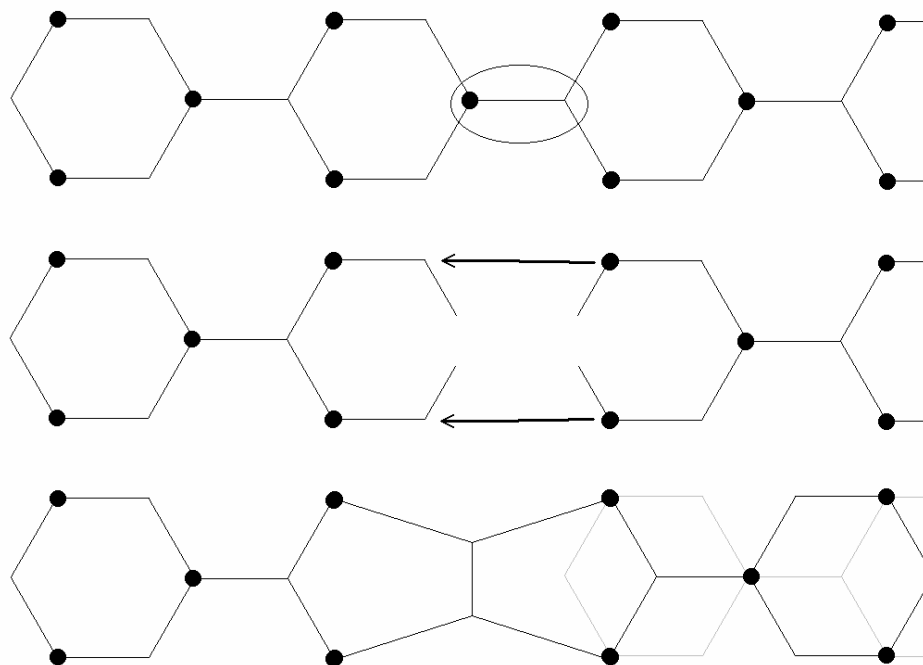


**Figure 2.11** Illustration of how a stacking fault causes dimerization at the surface. Removal of one atom and its nearest neighbor from the Si(111) surface causes reduction of one dangling. This process forms one dimer and a shift of the lattice (relative to the unshifted positions marked in gray) called a stacking fault. Since the hexagons in the shifted region switch surface atoms (black circles) for 2<sup>nd</sup> layer atoms (vertices) the positions of the surface atoms in the faulted region is unchanged – only the 2<sup>nd</sup> layer atoms are in different positions.

The first major structural information came from the STM studies of Binnig *et al.*<sup>42</sup>, which showed 12 protrusions inside the unit cell, and deep holes in the corners. Ion scattering studies<sup>43</sup> carried out by Tromp *et al.*<sup>44</sup> and Culbertson *et al.*<sup>45</sup> found evidence for substantial rearrangement in the subsurface layers, which supported the stacking-fault model where large sections of the silicon surface layers would be shifted a fraction of a unit cell relative to the bulk positions.

Takayanagi *et al.*<sup>46</sup> proposed the currently accepted model of the Si(111)  $7\times 7$  reconstruction based on transmission electron diffraction. Called the dimer-atom-stacking-fault (DAS) model, it has several different features, which help to minimize the number of unpaired electrons dangling off the surface. One method of eliminating dangling bonds is to simply eliminate some of the atoms from the surface. Consider the following process illustrated in Figure 2.11. One atom with a dangling bond, and one of its nearest-neighbors (which is not actually on the surface) is removed from the surface. That leaves 4 atoms with unsatisfied bonds. However, if there is a half-cell shift of the atoms of the underlying layer, then the 4 atoms can bond with each other as shown in Figure 2.11, and there are finally only two unsatisfied bonds left in the subsurface layer. The two atoms with the unsatisfied bonds can form a dimer. The Si(111)  $7\times 7$  surface is cross-hatched with rows of these dimers, and associated shifting of the atoms in the subsurface layer. (STM images<sup>47</sup> indicate that  $7\times 7$  domains actually do form by the sudden formation of small regions of shifted atoms surrounded by dimers.)

When dimers chains with different orientations converge near the corners of the  $7\times 7$  unit cell, the cumulative effect of the stacking faults creates a spot where no bonds are available for an atom, which would normally be there. Thus one atom from the layer below the dimers has a dangling bond, which explains the deep holes seen by the STM images at the corners of the  $7\times 7$  cells. Since the dimer chains create such an unstable configuration when they converge, there is an energetic push to minimize the number of such zones. This promotes the large size of the  $7\times 7$  cell. If the dimer chains

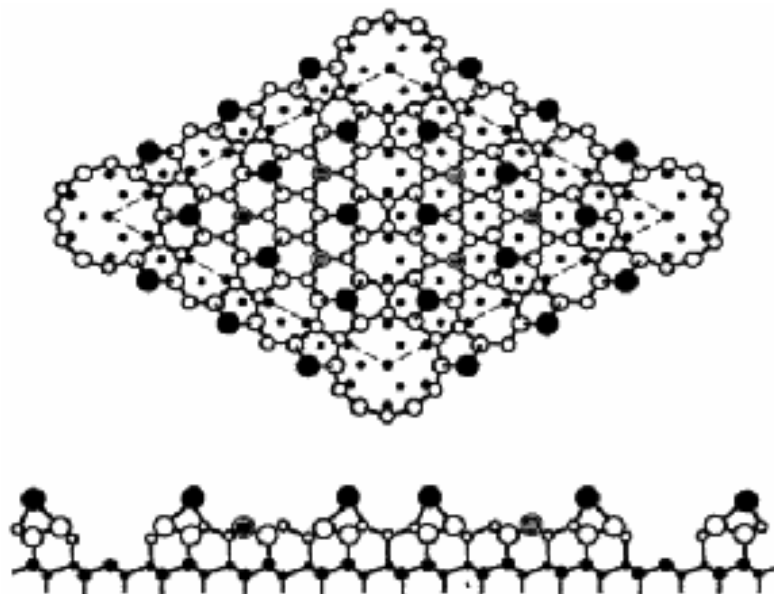


**Figure 2.12<sup>48</sup> Ball-and-stick model of the Si(111) 7×7 Dimer-Adatom-Stacking-fault (DAS) reconstruction. Top panel shows the surface, bottom panel shows cutaway view along the long diagonal of the unit cell. Large black circles are adatoms, gray spheres are rest atoms, and the unit cell is marked by dashed lines. The adatoms, rest atoms, and isolated corner atoms have one dangling bond each.**

don't cross, however, the total number of dimers decreases, which is also energetically unfavorable. (Metastable 9×9 and other unit cells have been observed, but they always relax into the 7×7 configuration.<sup>49</sup>) The stable 7×7 cell has groups of three dimers in a row before each crossing. This creates a unit cell with an edge length of 6 dimer atoms and one corner dangling bond for a total of 7 atoms and a 49 atom unit cell.

The regions between the rows of dimers have 21 atoms arranged into equilateral triangles with 6 atoms on an edge. There are two such triangles in each 7×7 unit cell, with one of the triangles in the usual position relative to the bulk structure, and one of the triangles in a faulted stacking position. The dangling bonds from triplets of neighboring

atoms in each triangle are satisfied by bonding to a single atom, called an adatom, which has only one dangling bond. There are twelve adatoms in each unit cell, which effectively reduces the number of dangling bonds from 43 to 19 in the following manner. The 12 adatoms, inside the unit-cell, cause the removal of 36 dangling-bonds in the first layer, but add 12 into the adatom layer. Thus, a net reduction of 24 is achieved. A stacking fault (in one half of the  $7\times 7$  unit-cell) allows for the reduction of dangling bonds by grouping atoms close enough for dimerization to occur along the edges of the  $7\times 7$  unit-cell and across the short unit-cell diagonal. Hence, dimerization further reduces the dangling-bond count by six. The final structure has only 19 ( $49-36+12-6$ ) dangling bonds, which stabilizes it. It is interesting to note that this process still leaves some residual instability. In an ideal situation the total number of dangling bonds could be cut to  $1/3^{\text{rd}}$  of the original value, whereas the  $7\times 7$  structure only cuts the number of dangling bonds to  $\frac{19}{49}$  or  $\sim 39\%$  of that for bulk termination.

For experimental purposes, the  $7\times 7$  structure can be easily identified by its distinctive LEED pattern (see Figure 2.13). The bright primary spots in the corners are a fourier transform of the periodicity of the  $1\times 1$  unit cell of the bulk-terminated surface. The 6 fainter spots along each edge are due to the  $7\times 7$  reconstruction. (Some faint spots inside the triangles can also be made out at some energies.)

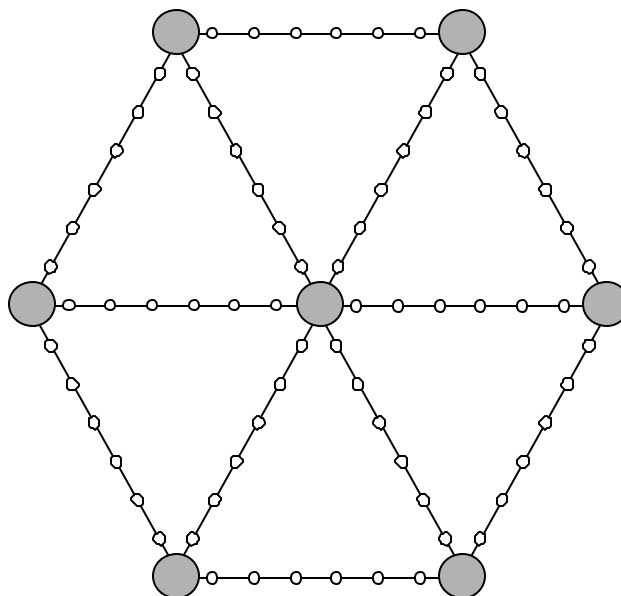


**Figure 2.13** LEED diagram for the **Si(111) 7×7** surface. (Note the 3-fold symmetry, where the alternating lines of the hexagon are not equivalent.). For the sake of simplicity only the spots lying along the principle axes of symmetry are depicted.

#### **2.4-c Prior Investigations of the Cs/Si(111)-7×7 Interface**

The adsorption of cesium onto the Si(111) 7×7 surface has not been studied as intensively as the adsorption onto the Si(100) 2×1 surface. However, a number of studies have been carried out, primarily focussing experimental<sup>50,51</sup> and theoretical<sup>52</sup> efforts on the sub-saturation regime where the interface is found to have various degrees of order. Many issues remain to be answered for this system, including the saturation coverage, which, once again, is disputed.



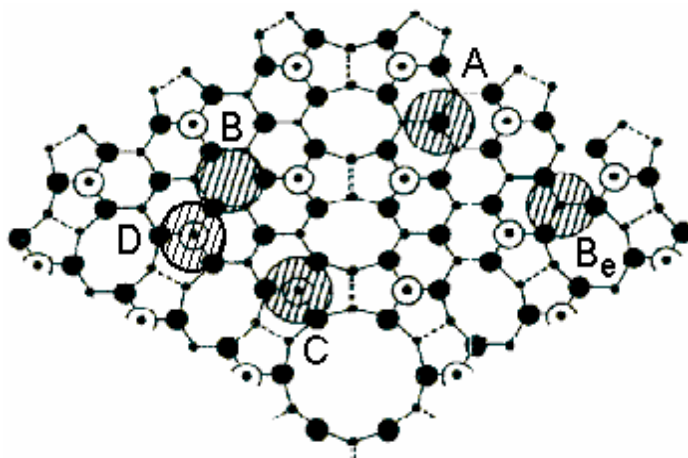


**Figure 2.14** Proposed binding sites for cesium on the Si(111)  $7\times 7$  surface. Solid circles: silicon atoms, open circles: silicon adatoms, hatched circles: cesium atoms (not to scale). A: on top of a rest atom, B: threefold coordinated hollow site,  $B_e$ : threefold coordinated eclipsing site, C: on top site for corner adatom, and D: on top site for inner adatom.<sup>53</sup>

Figure 2.14 shows the various proposed binding sites for cesium on the  $7\times 7$  reconstruction. Site A is on top of a rest atom. There are 6 such sites in the  $7\times 7$  cell. Site B is the threefold-coordinated (*i.e.* the three closest atoms are equally spaced around this site). There are only two such sites on the  $7\times 7$  cell.  $B_e$  is also threefold-coordinated, but it eclipses an atom in the surface just below it. There are 9 such sites in each cell. C is the site directly on top of a corner adatom (6 sites), and D is the site directly on top of an inner adatom (6 sites).

Magnusson *et al.*<sup>54,55</sup> found, based on UPS and angle-resolved inverse photoemission that cesium first adsorbs onto the adatom dangling bonds (sites C and D in Figure 2.14). Hashizume *et al.* also found using FI-STM that 70% of the initial cesium atoms bond onto the adatoms on the faulted half of the substrate  $7\times 7$  cells, and they bond

to D atoms before C atoms.<sup>51</sup> A more recent STM study<sup>56</sup> also confirms the tendency to adsorb preferentially on the faulted half of the surface. Eteläniemi *et al.* found via x-ray standing waves that at saturation, mostly A, and B sites are filled, (plus 36% of the cesium atoms are in random sites possibly including some B<sub>e</sub> and a very small number C and D but largely other sites not specified) and the overall system is disordered.<sup>57</sup> They also report that occupation of the A and B type sites, should necessitate the removal of some of the adatoms from the silicon surface. Hansen *et al.* have shown via Second Harmonic Generation (SHG) that cesium will stick to a sample after room temperature saturation coverage is reached, as long as cesium is being dosed. As soon as the dosing stops, however, the cesium coverage rapidly returns to the saturation level.<sup>58</sup>

The LEED pattern from the room temperature saturation coverage is very blurry 7×7, with a large background.<sup>55</sup> A short annealing at 300° sharpens up the 7×7 signal, but also removes much of the adsorbed cesium.<sup>57</sup> With so many different bonding site possibilities, most of the long-range order in the unannealed surface is destroyed, leaving behind essentially a 1×1 LEED image.

In any case, the coverage of the room temperature saturation state is not established. Eteläniemi *et al.* predict saturation at 0.48 and 0.61 monolayers.<sup>57</sup> Their conclusions, however, are highly dependent on their models, which fail to account for the positions of many of the cesium atoms. Magnusson *et al.* report room temperature saturation has all the dangling bonds except the corner hole filled or  $\frac{18}{49} = 0.367$  ML.<sup>54</sup>

The question of coverage is essential to understanding the metallization of the Cs/Si(111)  $7\times 7$  interface. The saturation coverage is reported variously as a metal<sup>59,54</sup> and as a semiconductor.<sup>55</sup> The key factor in understanding metallization is to know how far apart the cesium atoms are. If they are close enough for overlap between their electron clouds, then the surface is expected to be metallic. If they are farther apart, then the surface is expected to be a semiconductor. (The distance between cesium atoms in pure cesium bulk is 5.24 Å, but the effective radius may be different on the silicon surface.) RBS can provide crucial insight into this complicated interface. A low coverage will imply a tendency to favor certain adsorption sites over others but at the same time leave more room open for a disordered surface. A high coverage on the other hand implies a more ordered surface.

#### **2.4-d The Si(111)( $\sqrt{3} \times \sqrt{3}$ )R30°-B Reconstruction**

The previous discussions focused on reconstructions of elemental Si surfaces. A whole new set of reconstructions can also be obtained by introducing small amounts of impurities or dopants to the surface. The Si(111) surface is a good candidate for observing the effects of dopants and yields a variety of reconstructions. The simplest reconstruction, which can be visualized is one where each dangling bond per surface unit cell is satisfied by dopant X, or in other words, a  $1\times 1$ -X surface unit cell. However it has been determined from experiments that most dopant-induced reconstructions will involve longer range reordering of the surface. This is primarily due to the electronic properties

of the dopant atom. The reordering also depends to a large degree on the surface temperature and the post-deposition annealing and contamination parameters.

The most common dopant-induced reconstruction forms a  $\sqrt{3} \times \sqrt{3}$  surface unit cell. This reconstruction can be induced by several different impurities, the most notable being the group III elements In, Ga, Al, and B.<sup>60</sup> Some metals also diffuse into the bulk to form silicide compounds. In contrast, the reconstruction induced by the group III elements, is a surface phenomenon. Unlike the other group III elements, the lightest among them, boron, diffuses into the subsurface layer,<sup>61, 62, 63, 64, 65, 66, 67</sup> but does not diffuse into the bulk. The surface is stable and well ordered and can be thought of as an archetypical model surface. It is typically obtained by obtaining a clean Si(111)  $7 \times 7$  surface followed by boron deposition and annealing.<sup>61, 62</sup>

The surface layer of Si has several positions of high symmetry, which are potential binding sites for the adsorbate atoms. These are called the T1, T4, H3, and B5 sites shown in Figure 2.15, and Figure 2.16. The first goal to gain an understanding of these structures is to determine the absolute coverage followed by the position of the adsorbed boron atoms and relaxation of the surface layers. The models can be corroborated by experiments and theoretical calculations to determine the most stable structures.

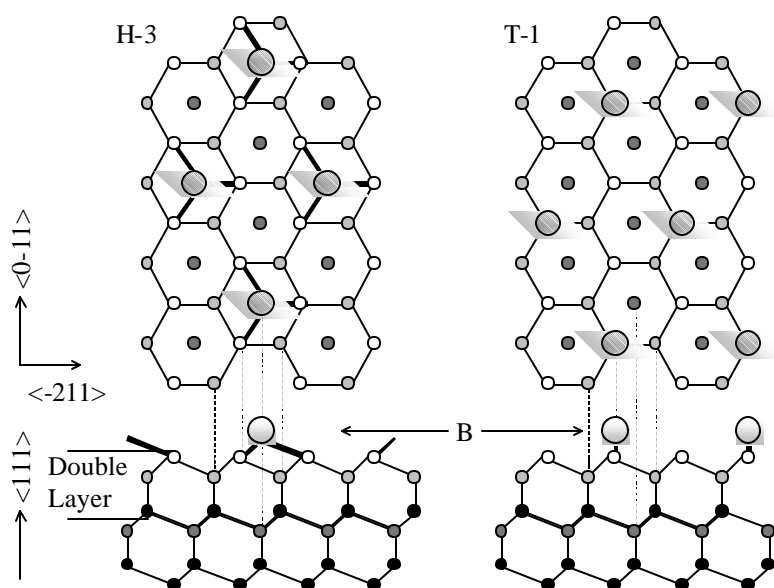


Figure 2.15 Top and side view showing the H-3 and T-4 adsorption sites.

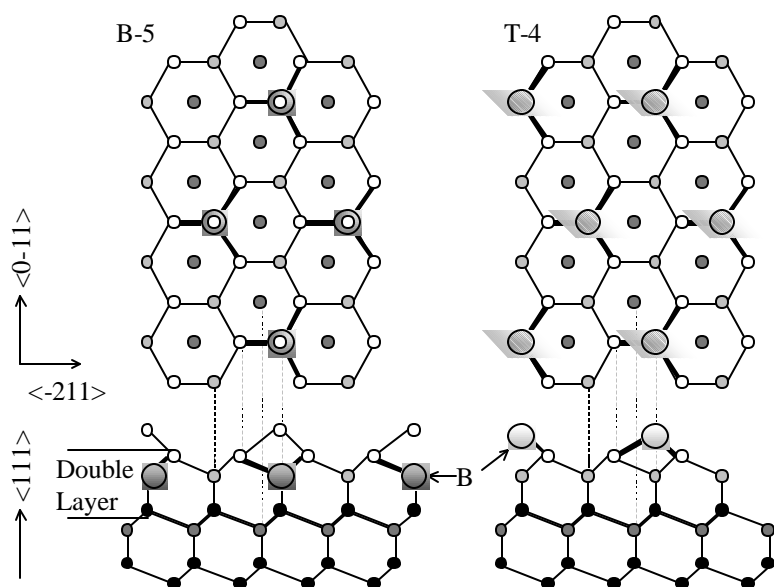


Figure 2.16 Top and side view showing the B-5 and T-4 adsorption sites

The lowest adsorbate coverage of  $1/3^{\text{rd}}$  ML corresponds to only one of the high symmetry sites containing a dopant atom followed by  $2/3^{\text{rd}}$  ML  $3/3^{\text{rd}}$  ML, and finally  $4/3^{\text{rd}}$  ML where all the high symmetry sites are occupied. If we compare with the  $7\times 7$  surface LEED studies of the newly reconstructed  $\text{Si}(111)(\sqrt{3}\times\sqrt{3})\text{R}30^\circ\text{-B}$  surface exhibits a  $30^\circ$  rotation of the axis of symmetry and a disappearance of the long range order spots corresponding to the  $7\times 7$  surface.

As discussed earlier RBS and STM are in general the best techniques for making coverage measurements and investigating surface structure. However, for boron, RBS is not a good probe. The boron atom is too light and its signature is lost in the RBS signal corresponding to the bulk substrate. STM experiments have shown silicon sitting at an adatom position on the topmost Si double layer<sup>61, 63, 67</sup> also implying that boron diffuses into the subsurface layer during annealing. In fact, recent STM studies<sup>67</sup> show that B attaches at first to the T-4 site and diffuses into the bulk B-S5 position only after annealing. Detailed LEED of the surface was compared with simulation of LEED patterns for the four likely reconstructions outlined above. There was good agreement with the B-S5 model.<sup>68</sup> Keating energy analysis of the surface structures also pointed at the B-S5 surface as the lowest in energy.

The best model that fits this scenario, is one where boron attaches at the unique B-S5 subsurface site and the Si adatom sits at the T4 site just above boron, implying a  $1/3^{\text{rd}}$  ML coverage for boron. In this model, charge transfer is expected from Si adatom sitting at the T4 site, to the substituted B atom directly below in the B-S5 site resulting in an

empty dangling bond. This is because the trivalent B atom is forced to form four covalent bonds instead of three. Such a charge transfer was verified from STM measurements.<sup>65</sup> Further support for the structure came from k-resolved inverse photoemission and angle resolved photoemission spectroscopy by Grehk et al.<sup>62</sup> Their studies showed evidence for surface states corresponding to the empty dangling bond, the backbond pointing back at the surface and also the bonds between the boron and the 3 neighboring subsurface atoms. Scanning Tunneling Spectroscopy (STS) by Avouris et al., also showed similar evidence for unoccupied and occupied bands corresponding to the dangling bond and the backbond respectively.<sup>66</sup> The picture was further supported by total energy calculations of the surface, which showed that the BS5 position was the most favored site for boron adsorption.<sup>61, 64</sup>

#### **2.4-e Prior Investigations of the Cs/Si(111)( $\sqrt{3} \times \sqrt{3}$ )R30°-B Interface**

Along with the other alkali metal Si interfaces the Cs/Si(111)( $\sqrt{3} \times \sqrt{3}$ )R30°-B has been subjected to various surface probes. Work function change studies at room temperature, conducted by Chen<sup>4</sup> show that in contrast with the Na or K adsorbed Si(111)( $\sqrt{3} \times \sqrt{3}$ )R30°-B interface, which remain semiconducting on reaching saturation, the Cs/Si(111)( $\sqrt{3} \times \sqrt{3}$ )R30°-B interface is metallic. This is supported further by very detailed and in depth studies also by Chen et al.<sup>4</sup> using electron energy loss spectroscopy (EELS) angle resolved photoelectron spectroscopy (ARPES) and other photoemission studies. ARPES reveals surface states, which remain just below Fermi

level at all coverages beam energies and incidence angles for the Na and K saturated surfaces. Corresponding core level spectroscopy reveals behavior consistent with that seen in other non metallic interfaces. EELS loss features lend further support to the semiconducting nature of the surface. In contrast for Cs interface there is a perceptible dip in the work function change just before saturation, which is associated with metallization. EELS ARPES and core level photoemission studies all support this view.

An understanding of metallization can be achieved by proposing a structural model for the interface, and see how it fits in with the observed phenomenon. LEED studies have shown us that the surface periodicity remains the same on alkali metal deposition suggesting that there is minimal rearrangement of the surface.<sup>68</sup> It is thus very likely that the alkali-metals simply attach themselves to all the empty dangling bond sites as shown in Figure 2.17. A difference in the atomic radii can account for the differing properties of the 3 surfaces. Cesium having the largest radius gives rise to a metallic interface because it is easier for valence electrons to transfer from one atom to another. The RBS measurement of saturation coverage for this interface will be a direct verification of a most significant aspect of this model, its coverage.



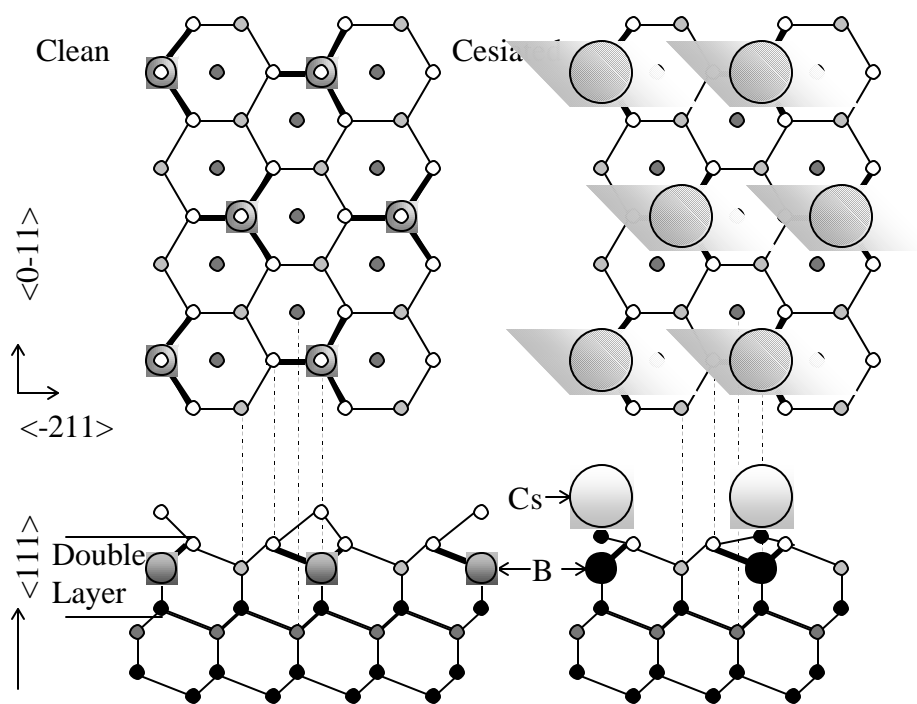


Figure 2.17 Proposed model of Cs/Si(111)( $\sqrt{3} \times \sqrt{3}$ )R30°-B surface.

## List of References

- <sup>1</sup> N. Ashcroft and N. D. Mermin, *Solid State Physics* (Saunders College, Philadelphia, 1976)
- <sup>2</sup> A crystal cleaved or otherwise prepared so as to expose a plane perpendicular to the vector (1,0,0) is called Si(100).
- <sup>3</sup> A. Zangwill, *Physics at Surfaces* (Cambridge University Press, Cambridge, 1988).
- <sup>4</sup> J. Chen, Ph.D. dissertation, University of Pennsylvania, 1994.
- <sup>5</sup> I. H. Hong, S. C. Shyu, Y. C. Chou, and C. M. Wei, *Phys. Rev. B* **52**, 16884
- <sup>6</sup> J. E. Klepeis and W. A. Harrison, *J. Vac. Sci. Technol.* **B7**, 964(1989).
- <sup>7</sup> R. M. Feenstra, *J. Vac. Sci. Technol.* **B7**, 925(189).
- <sup>8</sup> O. Pankratov and M. Scheffler, *Phys. Rev. Lett.* **70**, 351(1993).
- <sup>9</sup> G. A. Allan and M. Lanoo, *Surf. Sci.* **63**, 11(1977).
- <sup>10</sup> J. E. Northrup, J. Ihm, and M. L. Cohen, *Phys. Rev. Lett.* **47**, 1910(1981).
- <sup>11</sup> W. A. Harrison *Phys. Rev.* **B31**, 2121(1985).
- <sup>12</sup> C. B. Duke and W. K. Ford, *Surf. Sci.* **111**, L685(1981).
- <sup>13</sup> L. J. Whitman, J. A. Stroscio, R. A. Dragoset, and R. J. Celotta, *Phys. Rev.* **B44**, 5951(1991).
- <sup>14</sup> R. E. Schlier and H. E. Farnsworth, *J. Chem. Phys.* **30**, 917 (1959).
- <sup>15</sup> D. J. Chadi, *Phys. Rev. Lett.* **43**, 43 (1979).
- <sup>16</sup> A. I. Shkrebtii, R. Di Felice, C. M. Bertoni, and R. Del Sole, *Phys. Rev. B* **51**, 11201 (1995).
- <sup>17</sup> R. M. Tromp, R. J. Hamers, and J. E. Demuth, *Phys. Rev. Lett.* **55**, 1303 (1985).

- <sup>18</sup> E. Landemark, C. J. Karlsson, Y.-C. Chao, and R. I. G. Uhrberg, Phys. Rev. Lett. **69**, 1588 (1992).
- <sup>19</sup> R. J. Hamers, R. M. Tromp, and J. E. Demuth, Phys. Rev. B **34**, 5343 (1986).
- <sup>20</sup> After P. Castrucci, S. Lagomarsino, F. Scarinci and G. E. Franklin, Phys. Rev. B **51**, 5043 (1995)
- <sup>21</sup> B. Goldstein, Surf. Sci. **35**, 227 (1973).
- <sup>22</sup> J. D. Levine, Surf. Sci. **34**, 90 (1973).
- <sup>23</sup> P. S. Mangat and P. Soukiassian, Phys Rev. B **52**, 12020 (1995).
- <sup>24</sup> Y.-C. Chao, L. S. O. Johansson, and R. I. G. Uhrberg, Phys Rev. B **54**, 5901 (1996).
- <sup>25</sup> H. Xu, H. Hashizume, and T. Sakurai, Phys. Stat. Sol. A **151**, 329 (1995).
- <sup>26</sup> Y. Enta, T. Kinoshita, S. Suzuki, and S. Kono, Phys. Rev. B **36**, 9801 (1987).
- <sup>27</sup> Y. Enta, T. Kihoshita, S. Suzuki, and S. Kono, Phys Rev B **39**, 1125 (1989).
- <sup>28</sup> A technique where x-rays excite surface atoms to emit core level electrons which then diffract from the grating formed by the other nearby atoms.
- <sup>29</sup> T. Abukawa and S. Kono, Phys. Rev. B **37**, 9097(1988).
- <sup>30</sup> T. Abukawa, T. Okane and S. Kono, Surf. Sci. **256**, 370 (1991).
- <sup>31</sup> T. Abukawa, T. Okane and S. Kono, Surf. Sci. **214**, 141 (1989).
- <sup>32</sup> LEED I-V is the analysis of how electron diffraction spot intensity (I) varies as the incident beam voltage (V) is varied.
- <sup>33</sup> H. Hamamatsu, H. W. Yeom, T. Yokoyama, T. Kayama, and T. Ohta, Phys. Rev. B **57**, 11883 (1998)
- <sup>34</sup> S. Kennou, M. Kamaratos, S. Ladas, and C. A. Papageorgopoulos, Surf. Sci. **216**, 462 (1989).
- <sup>35</sup> S. Tanaka, N. Takagi, N. Minami, and M. Nishijima, Phys. Rev. B **42**, 1868 (1990).

- <sup>36</sup> D. Jeon, T. Hashizume, and T. Sakurai, *J. Vac. Sci. Technol. B* **12**, 2044 (1994).
- <sup>37</sup> S. Arekat, S. D. Kevan, and G. L. Richmond, *Europhys. Lett.* **22**, 377 (1993).
- <sup>38</sup> A. J. Smith, W. R. Graham, and E. W. Plummer, *Surf. Sci. Lett.* **243**, L37 (1991).
- <sup>39</sup> P. Soukiassian, (Private communication).
- <sup>40</sup> K.D. Brommer, M. Needels, B.E. Larson, and J.D. Joannopoulos, *Phys. Rev. Lett.* **68** 1355 (1992).
- <sup>41</sup> I. Stich, M.C. Payne, R.D. King-Smith, J.S. Lin, and L.J. Clarke, *Phys. Rev. Lett.* **68** 1351 (1992).
- <sup>42</sup> G. Binnig, H. Rohrer, C. Gerber and E. Weibel, *Phys. Rev. Lett.* **50**, 120 (1983).
- <sup>43</sup> Various ion scattering techniques analyze variations in scattered ion intensities as a function of angle and energy to determine the structure and chemical composition of surfaces.
- <sup>44</sup> R. M. Tromp, E. J. van Loenen, M. Iwami, and F. W. Saris, *Solid State Commun.* **44**, 971 (1982).
- <sup>45</sup> R. J. Culbertson, L. C. Feldman, and P. J. Silverman, *Phys. Rev. Lett.* **45**, 2043 (1980).
- <sup>46</sup> K. Takayanagi, Y. Tanishiro, M. Takahashi, and S. Takahashi, *J. Vac. Sci. Technol. A* **3**, 1502(1985); *Surf. Sci.* **164**, 367(1985).
- <sup>47</sup> T. Hoshino, K. Kumamoto, K. Kokubun, and T. Ishimaru, *Phys. Rev. B* **51**, 14594 (1995).
- <sup>48</sup> H. Lim, K. Cho, I. Park, and J. D. Joannopoulos, *Phys. Rev. B* **52**, 17231 (1995).
- <sup>49</sup> K. Kumamoto, T. Hoshino, K. Kokubun, T. Ishimaru, and I. Ohdomari, *Phys. Rev. B* **53**, 12907 (1996)
- <sup>50</sup> T. Hashizume, K. Motai, Y. Hasegawa, I. Sumita, H. Tanaka, S. Amano, S. Hyodo, and T. Sakurai, *J. Vac. Sci. Technol. B* **9**, 745 (1991).

- <sup>51</sup> T. Hashizume, Y. Hasegawa, I. Sumita, and T. Sakurai, Surf. Sci. **246**, 189(1991).
- <sup>52</sup> L. Stauffer, and C. Minot, Surface Science **331-333**, 606 (1995).
- <sup>53</sup> Based on image in V. Eteläniemi, E. G. Michel, and G. Materlik, Phys. Rev. B **44**, 4036 (1991).
- <sup>54</sup> K. O. Magnusson, S. Wiklund, R. Dudde, and B. Reihl, Phys. Rev. B **44**, 5657(1991).
- <sup>55</sup> K. O. Magnusson, and B. Reihl, Phys. Rev. B **41**, 12071 (1990).
- <sup>56</sup> Jun Yoshikawa, Shu Kurokawa, and Akira Sakai, Appl. Surf. Sci. **202-205**, 169-170 (2001).
- <sup>57</sup> V. Eteläniemi, E. G. Michel, and G. Materlik, Phys. Rev. B **44**, 4036 (1991).
- <sup>58</sup> P-E. Hansen, K. Pedersen, L. Liu, and P. Morgen, Surf. Sci. **391**, 252 (1997).
- <sup>59</sup> H. H. Weittering , J. Chen, R. Pérez-Sandoz, and N. J. DiNardo, Surf. Sci. **307-309**, 978 (1994).
- <sup>60</sup> See for example, J. M. Nicholls, B. Reihl, and J. E. Northrup, Phys. Rev. B. **35**, 4137(1987).
- <sup>61</sup> I. W. Lyo, E. Kaxiras, and Ph. Avouris, Phys. Rev. Lett. **63**, 1261(1989).
- <sup>62</sup> T. M. Grehk, P. Mårtensson, J. M. Nicholls, Phys. Rev. **B46**, 2357(1992).
- <sup>63</sup> P. Bedrossian, R. D. Meade, K. Mortensen, D. M. Chen, J. A. Golovchenko, and D. Vanderbilt, Phys. Rev. Lett. **63**, 1257(1989).
- <sup>64</sup> E. Kaxiras, K. C. Pandey, F. J. Himpsel, and R. M. Tromp, Phys. Rev. B. **41**, 1262 (1990).
- <sup>65</sup> Ph. Avouris and R. Wolkow, Phys. Rev. **B39**, 5091(1989); Phys. Rev. Lett. **60**, 1049 (1988).
- <sup>66</sup> Ph. Avouris, I. W. Lyo, F. Bozso, and E. Kaxiras, J. Vac. Sci. Technol. **A8**, 3405 (1990).

<sup>67</sup> T. Stimpel, J. Schulze, H.E. Hoster, I. Eisele, H. Baumgartner, Applied Surface Science **162**, 384 (2000)

<sup>68</sup> J. E.Quinn, Ph.d. dissertation, State University of New York at stoneybrook, 1992